IL-10 dampens antitumor immunity and promotes liver metastasis via PD-L1 induction

Ahmad Mustafa Shiri, Tao Zhang, Tanja Bedke, Dimitra E. Zazara, Lilan Zhao, Jöran Lücke, Morsal Sabihi, Antonella Fazio, Siwen Zhang, Daniele V.F. Tauriello, Eduard Batlle, Babett Steglich, Jan Kempski, Theodora Agalioti, Mikołaj Nawrocki, Yang Xu, Kristoffer Riecken, Imke Liebold, Leonie Brockmann, Leonie Konczalla, Lidia Bosurgi, Baris Mercanoglu, Philipp Seeger, Natalie Küsters, Panagis M. Lykoudis, Asmus Heumann, Petra C. Arck, Boris Fehse, Philipp Busch, Rainer Grotelüschen, Oliver Mann, Jakob R. Izbicki, Thilo Hackert, Richard A. Flavell, Nicola Gagliani, Anastasios D. Giannou, Samuel Huber

Table of contents

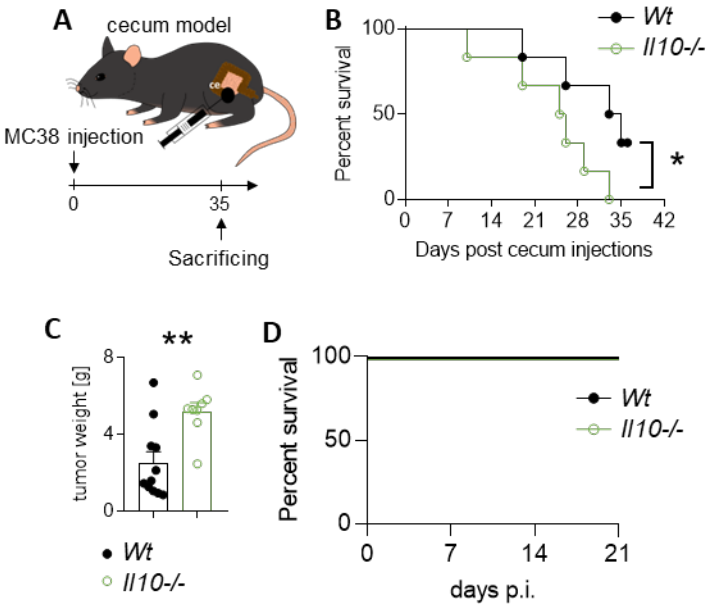

Fig. S1: *Il10*-deficiency in mouse promotes primary tumor growth

(**A**) Schematic overview of the intracaecal injection of MC38 cancer cells for spontaneous liver metastasis induction. (**B**) Overall survival and (**C**) Primary tumor weight in the caecum of *Wt* and *Il10-/-* mice (n ≥ 8 mice per group). (**D**) Overall survival of the mice after intrasplenic injection of MC38 cells. Data are presented as mean ± SEM. Non-significant (ns): $p > 0.05$; *: $p \leq 0.05$; **: $p < 0.01$, as calculated by Mantel-Cox test or Mann-Whitney *U* test. p.i.: post injection

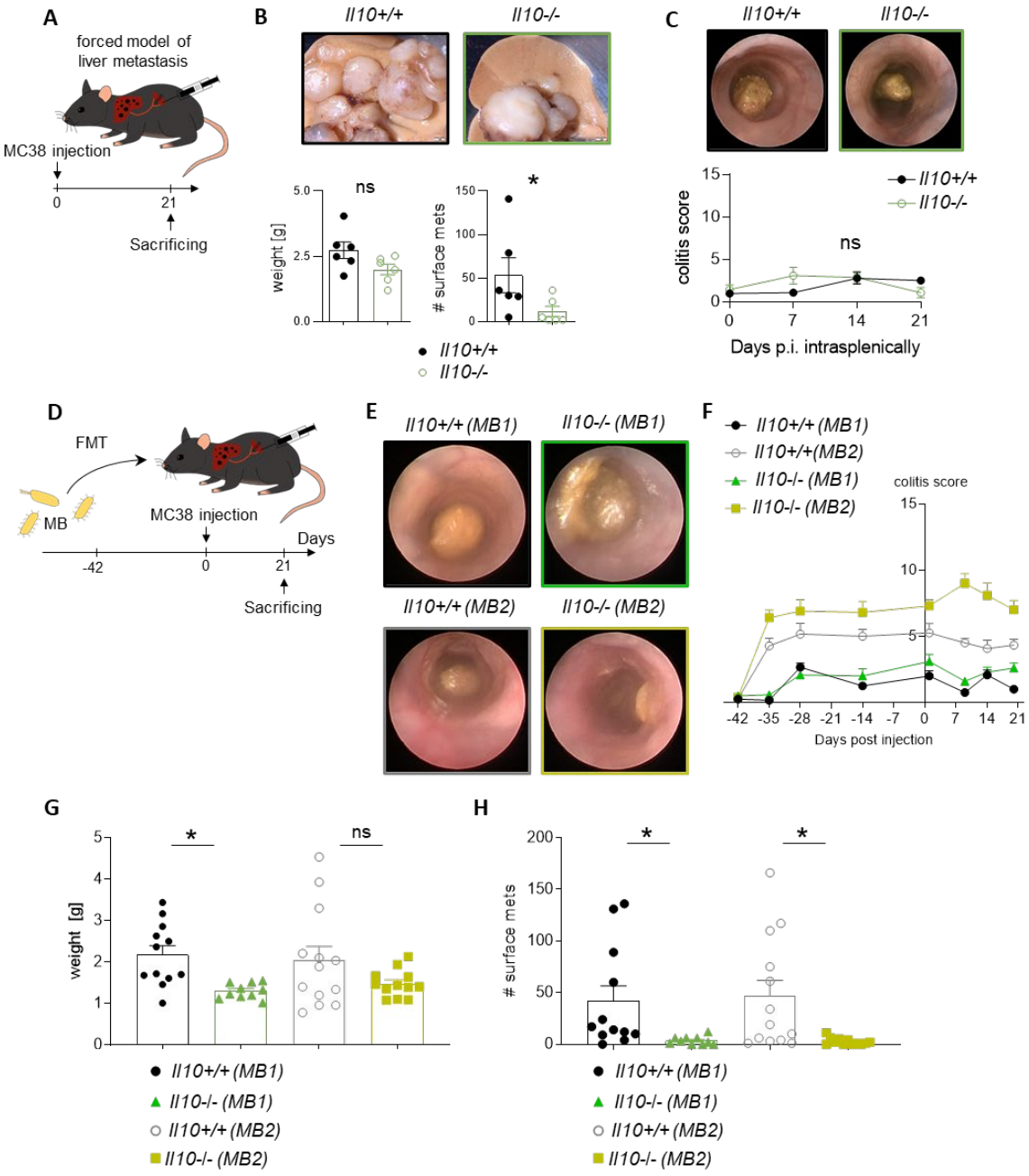

Fig. S2: The pathogenic role of IL-10 in liver metastasis formation is independent of colitis severity

(**A**) Schematic overview of the intrasplenic injection of MC38 cancer cells for forced liver metastasis induction in *Il10+/+* and *Il10-/-* littermates (n = 6 mice per group). (**B**) Representative pictures of liver metastasis, as well as analysis of liver weight and number of liver metastases. (**C**) Representative endoscopic view on day 21 and colitis score at different time points during liver metastasis formation. (**D**) Schematic overview of the i.s. injection of MC38 cancer cells for forced liver metastasis induction using *Il10+/+* and *Il10-/-* littermates following fecal microbiome (MB) transplant (*MB1, MB2*) (n ≥ 10 mice per group). (**E**) Representative endoscopic view of colon on day 21 post injection (i.s.) and (**F**) Colitis severity score at different time points during the whole

procedure. Livers were harvested and (**G**) liver weight as well as (**H**) number of microscopic liver metastases were analyzed. Scale bar: 2 mm. Data are presented as mean ± SEM. Non-significant (ns): $p > 0.05$; *: $p \leq 0.05$; **: $p < 0.01$, as calculated by Mann-Whitney *U* test or by one-way ANOVA with Bonferroni post hoc tests. FMT: fecal microbiome transfer.

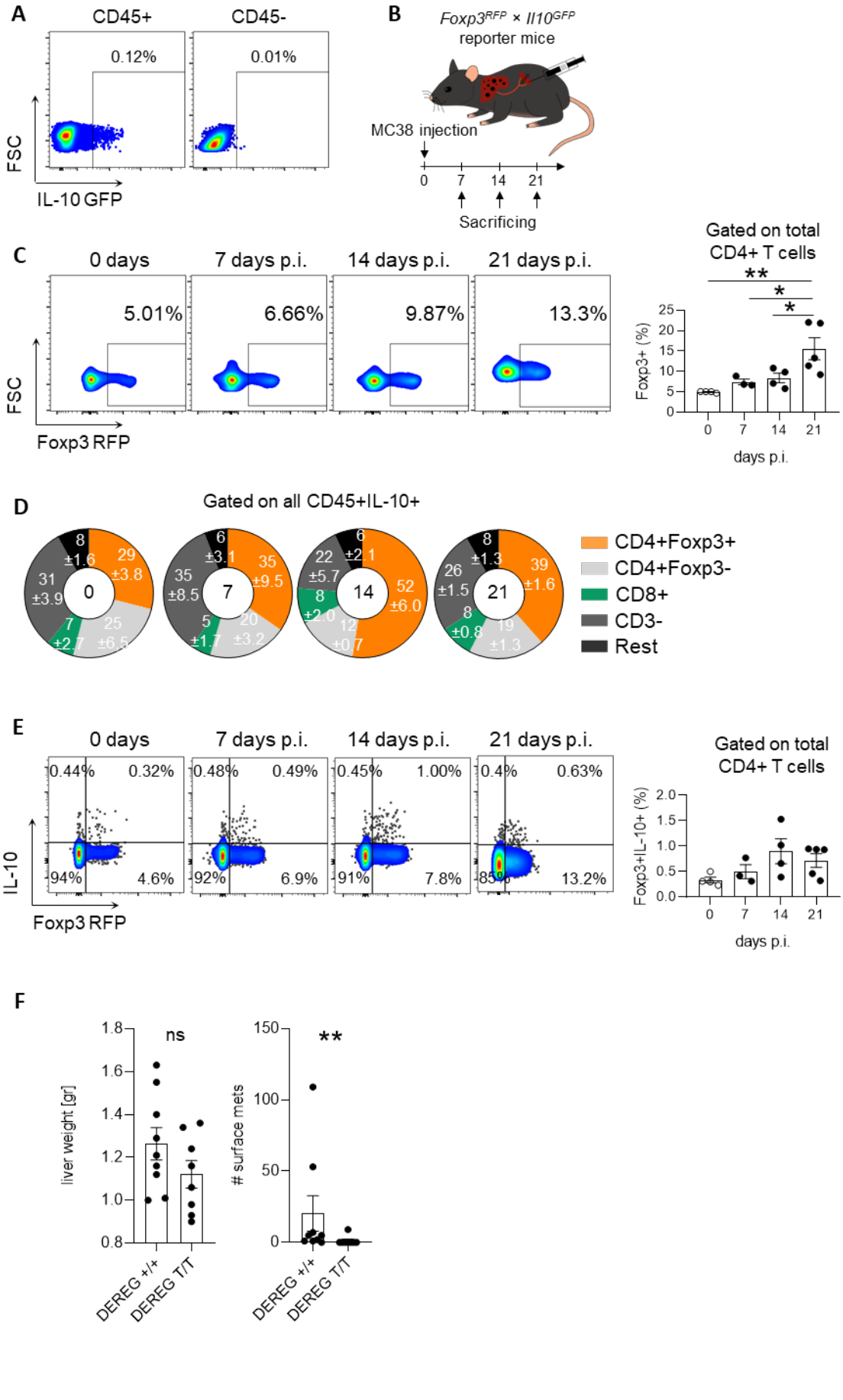
A
CD45+
CD45-
0.12%
0.01%
FSC
IL-10 GFP
B
Foxp3RFP × Il10GFP
reporter mice
MC38 injection
0
7
14
21
Sacrificing
C
0 days
7 days p.i.
14 days p.i.
21 days p.i.
5.01%
6.66%
9.87%
13.3%
FSC
Foxp3 RFP
Gated on total
CD4+ T cells
Foxp3+ (%)
days p.i.
D
Gated on all CD45+IL-10+
CD4+Foxp3+
CD4+Foxp3-
CD8+
CD3-
Rest
E
0 days
7 days p.i.
14 days p.i.
21 days p.i.
0.44%
0.32%
94%
4.6%
0.48%
0.49%
92%
6.9%
0.45%
1.00%
91%
7.8%
0.4%
0.63%
13.2%
IL-10
Foxp3 RFP
Gated on total
CD4+ T cells
Foxp3+IL-10+ (%)
days p.i.
F
ns
**
liver weight [gr]
surface mets
DEREG +/+
DEREG T/T

Fig. S3: Treg expansion together with a dynamic IL-10 increase are observed during liver metastasis formation

(**A**) IL-10 expression in hematopoietic and nonhematopoietic cells of a healthy mouse liver. (**B**) *Foxp3*^{RFP};*Il10*^{GFP} reporter mice received MC38 colon cancer cells i.s. and were sacrificed at the indicated time points (n ≥ 3 mice per group). (**C**) Frequency of Tregs within CD4+ T cells along metastasis formation. (**D**) General distribution of CD45+IL-10+ cells at the indicated timepoints. (**E**) IL-10 producing Tregs along metastasis formation. (**F**) *Wild type* and *DEREG* mice received i.s. of MC38 cells and livers were harvested in 21 days post injection. Liver weight (left) and number of liver metastasis (right) in mice with Treg depletion and their controls. Data are presented as mean ± SEM. Non-significant (ns): $p > 0.05$; *: $p \leq 0.05$; **: $p < 0.01$; ***: $p < 0.001$, as calculated by one-way ANOVA with Bonferroni post hoc tests.

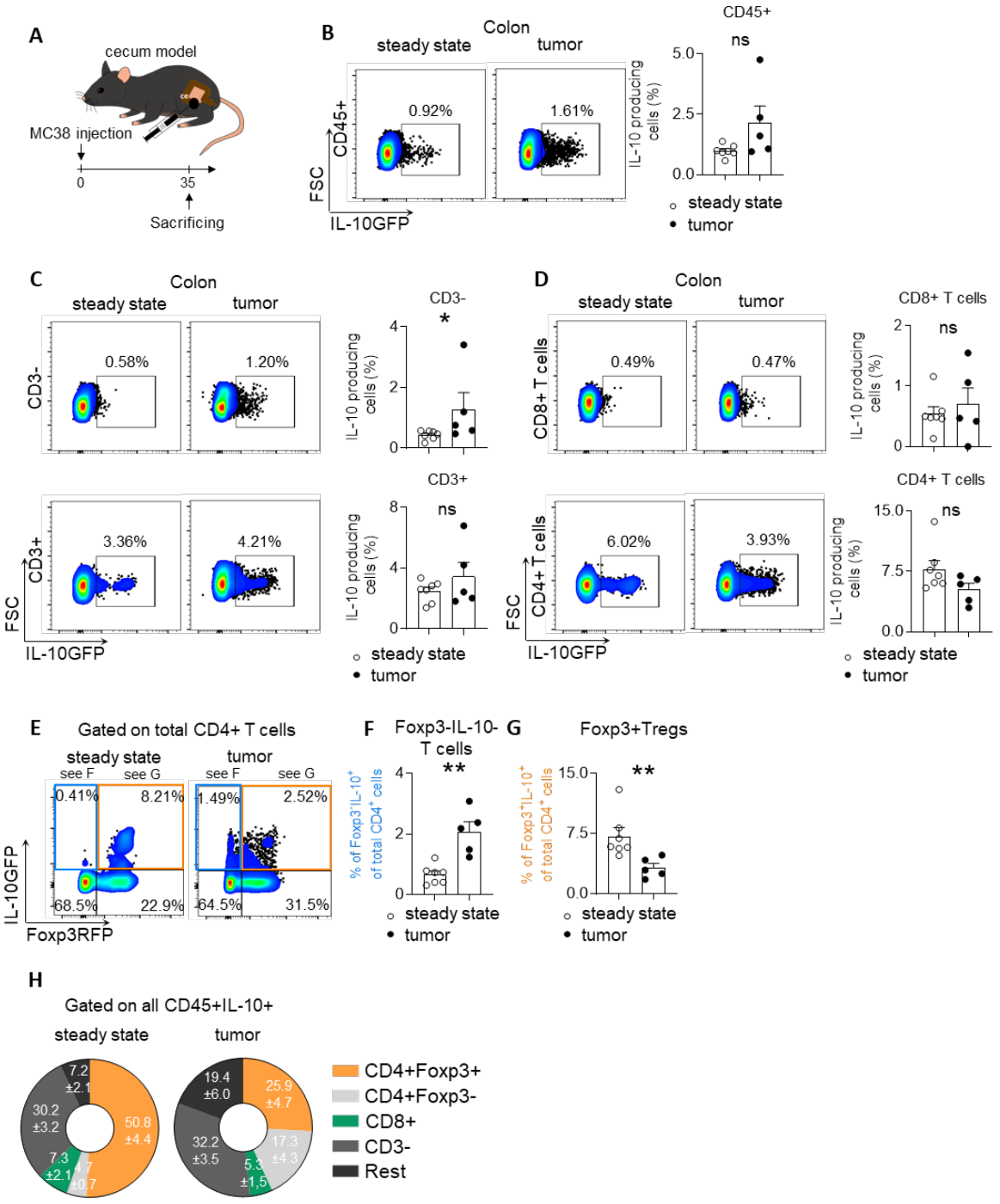

Fig. S4: Innate cells are the major source of IL-10 producing cells in CRC

(**A**) Schematic overview of the intracaecal injection of MC38 cancer cells for CRC induction in *Foxp3*^{RFP};*Il10*^{GFP} reporter mice (n ≥ 5 mice per group). Immune cells from cecum were then isolated and stained for flow cytometry 35 days post injection. The frequency of IL-10+ cells in the fraction of (**B**) CD45+ cells, (**C**) CD3- and T cells, and in (**D**) CD8+ T cells and CD4+ T cells was analyzed. (**E**) IL-10 expression in (**F**) Foxp3- IL-10+ T cells and (**G**) Foxp3+Tregs. (**H**) General distribution of all IL-10 producing CD45+ cells in healthy cecum and cecum tumor. Data are presented as mean ± SEM. Non-significant (ns): $p > 0.05$; *: $p \leq 0.05$; **: $p < 0.01$; ***: $p < 0.001$, as calculated by Mann-Whitney *U* test.

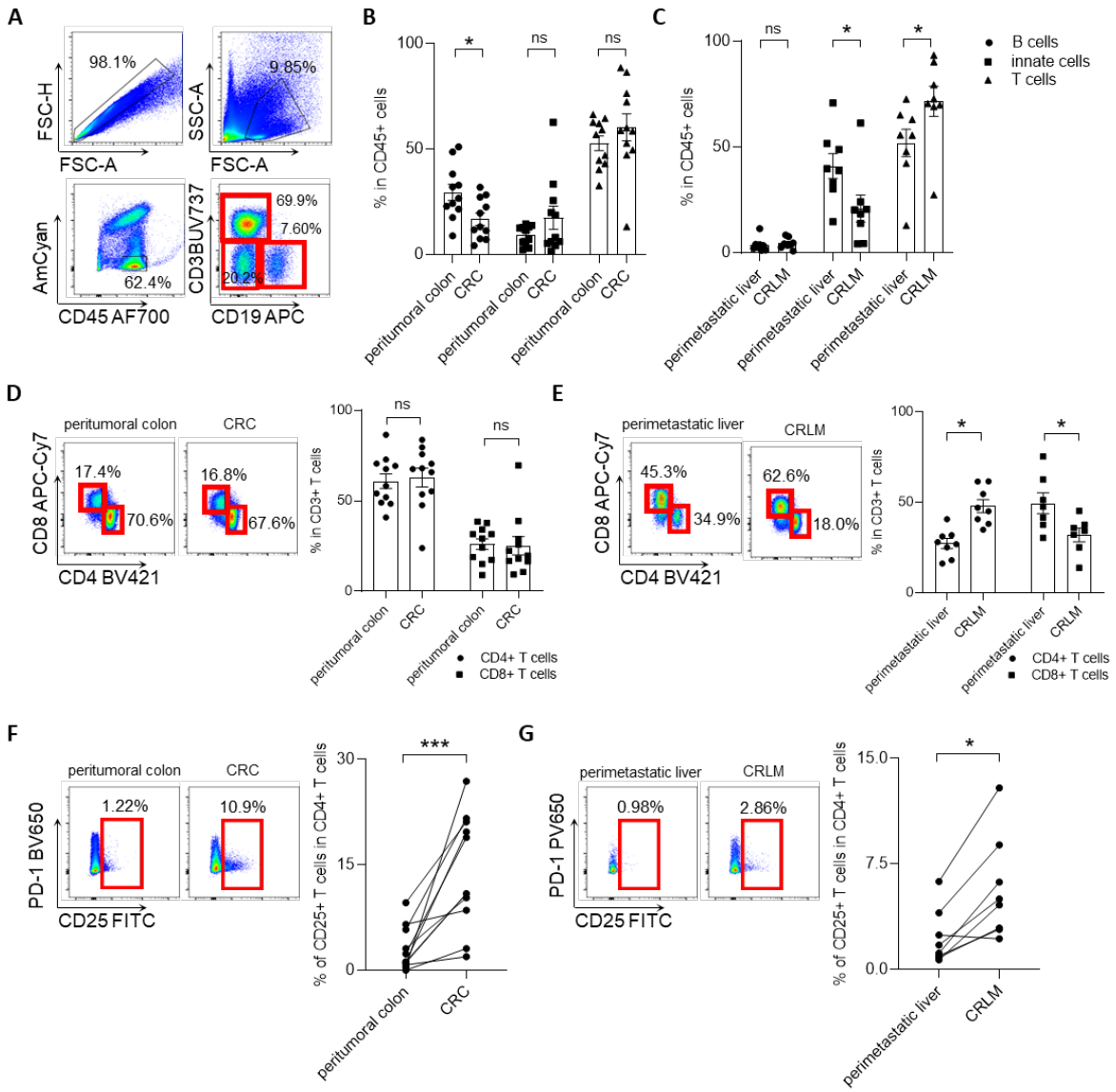

Fig. S5: Different immune cell compositions in CRC and CRLM. Immune cells were isolated from human CRC and CRLM, and subsequently stained for flow cytometry. (**A**) Gating strategy and analysis for B cells, innate cells and T cells in (**B**) CRC and (**C**) CRLM. (**D, E**) Representative FACS plots and analysis of CD4+ and CD8+ T cells in (D) CRC and (E) CRLM. (**F, G**) Representative FACS plots and analysis of CD4+CD25+ T cells in (D) CRC and (E) CRLM. Data are presented as mean ± SEM. Non-significant (ns): $p > 0.05$; *: $p \leq 0.05$; **: $p < 0.01$; ***: $p < 0.001$, as calculated by Mann-Whitney *U* test.

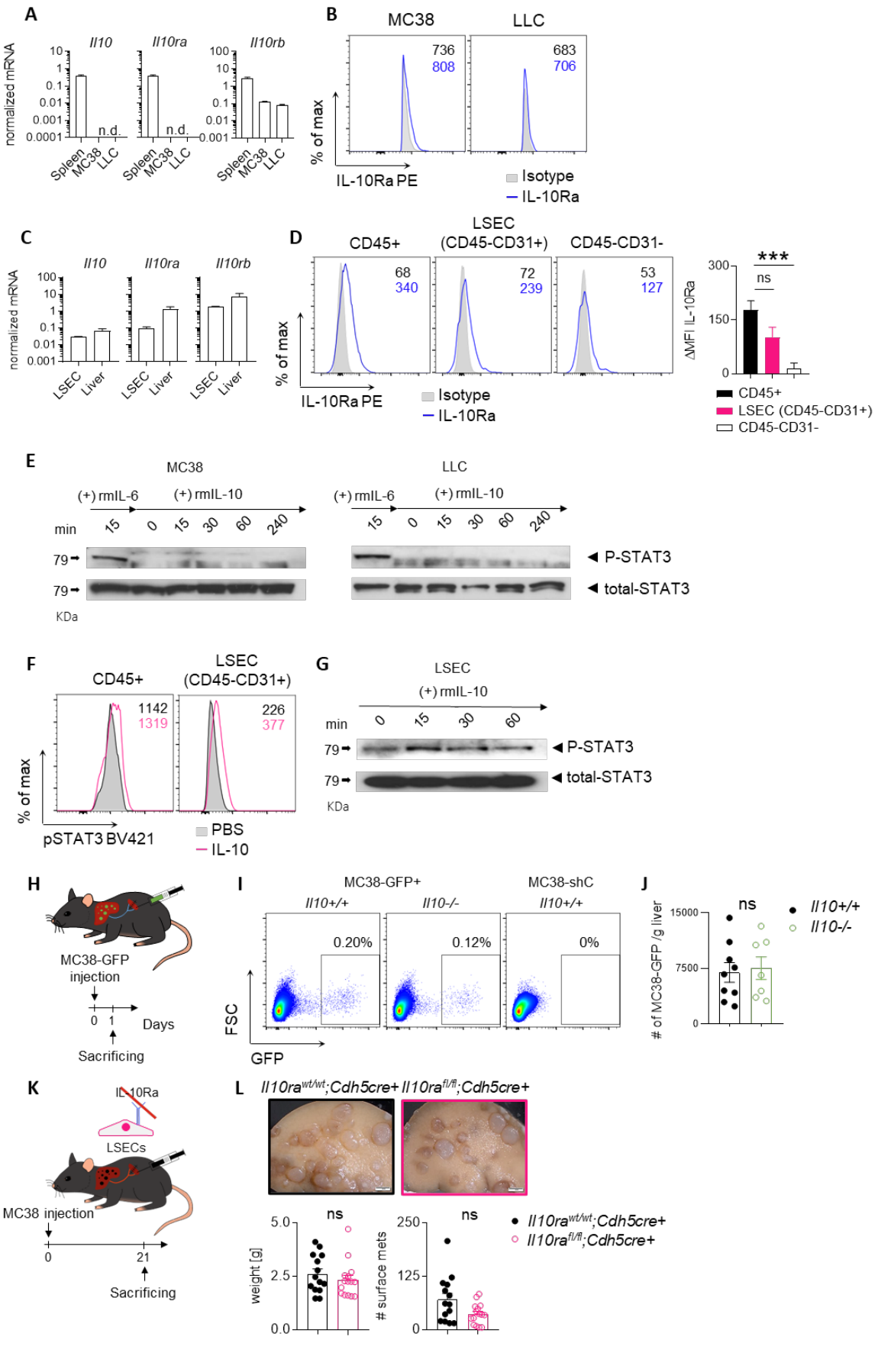
A
Il10
Il10ra
Il10rb
normalized mRNA
n.d.
Spleen
MC38
LLC
B
MC38
LLC
736
808
683
706
% of max
IL-10Ra PE
Isotype
IL-10Ra
C
Il10
Il10ra
Il10rb
normalized mRNA
LSEC
Liver
D
CD45+
LSEC (CD45-CD31+)
CD45-CD31-
68
340
72
239
53
127
% of max
IL-10Ra PE
Isotype
IL-10Ra
ΔMFI IL-10Ra
***
ns
CD45+
LSEC (CD45-CD31+)
CD45-CD31-
E
MC38
LLC
(+) rmIL-6
(+) rmIL-10
min
15
0
15
30
60
240
79
P-STAT3
total-STAT3
KDa
F
CD45+
LSEC (CD45-CD31+)
1142
1319
226
377
% of max
pSTAT3 BV421
PBS
IL-10
G
LSEC
(+) rmIL-10
min
0
15
30
60
79
P-STAT3
total-STAT3
KDa
H
MC38-GFP
injection
0
1
Days
Sacrificing
I
MC38-GFP+
MC38-shC
Il10+/+
Il10-/-
Il10+/+
0.20%
0.12%
0%
FSC
GFP
J
ns
Il10+/+
Il10-/-
# of MC38-GFP /g liver
15000
7500
0
K
IL-10Ra
LSECs
MC38 injection
0
21
Sacrificing
L
Il10ra^wt/wt;Cdh5cre+
Il10ra^fl/fl;Cdh5cre+
ns
weight [g]
5.0
2.5
0.0
ns
surface mets
250
125
0
Il10ra^wt/wt;Cdh5cre+
Il10ra^fl/fl;Cdh5cre+

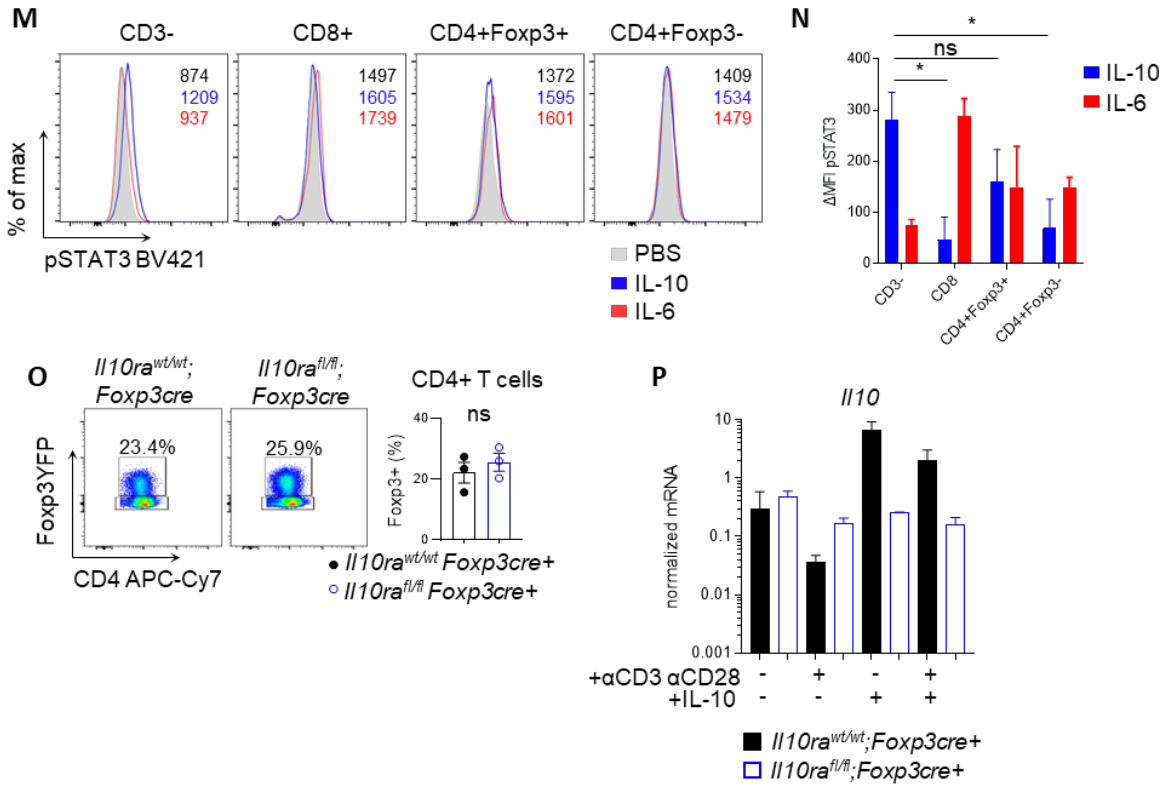

Fig. S6: IL-10 signaling in cancer cells and LSECs does not affect liver metastasis formation

(**A**) mRNA expression of the IL-10 and IL-10 receptor complex in MC38 and LLC cancer cells. (**B**) MFI of the IL-10Ra expression in MC38 and LLC cancer cells measured using flow cytometry. (**C**) mRNA expression of IL-10 and IL-10 receptor complex in total liver and LSECs isolated from *Wt* mice. (**D**) Quantification (ΔMFI) of IL-10Ra expression in total immune cells, LSECs and the rest of the cells isolated from *Wt* murine liver. (**E**) Phosphorylation of STAT3 in MC38 and LLC cancer cells upon *in vitro* IL-6 (10 ng/µl) or IL-10 (10 ng/µl) stimulation at indicated time points measured using Western Blot. (**F, G**) Phosphorylation of STAT3 in *Wt* LSECs after *in vitro* IL-10 stimulation (10 ng/µl) measured using (F) flow cytometry (after a 60-minute stimulation) or (G) Western blot (at indicated timepoints). (**H**) MC38-GFP cancer cells were intrasplenically injected into *Il10+/+* and *Il10-/-* littermates (n ≥ 7 mice per group). (**I**) Representative FACS-plot of extravasated MC38-GFP cells and (**J**) the number of extravasated MC38-GFP cells. (**K**) MC38 colon cancer cells were i.s. injected into mice with LSECs-specific IL-10Ra deletion and their littermate controls (n ≥ 12 mice per group). (**L**) Representative images, liver weight as well as number of liver metastasis were analyzed. (**M**) Representative FACS plot and (**N**) ΔMFI quantification of pSTAT3 staining in hepatic immune cells isolated from Wt mice upon IL-10 (10 ng/µl) or IL-6 (10 ng/µl) stimulation *in vitro*. (**O**) Hepatic Treg frequency within CD4+ T cells and (**P**) *Il10* level measured using qPCR upon IL-10 and/or antiCD3/CD28 stimulation *in vitro*. Scale bar: 2 mm. Data are presented as mean ± SEM. Non-significant (ns): $p > 0.05$; ***: $p < 0.001$, as calculated by Mann-Whitney *U* test or one-way ANOVA (Bonferroni) with Bonferroni post hoc tests. LSECs: liver sinusoidal endothelial cells.

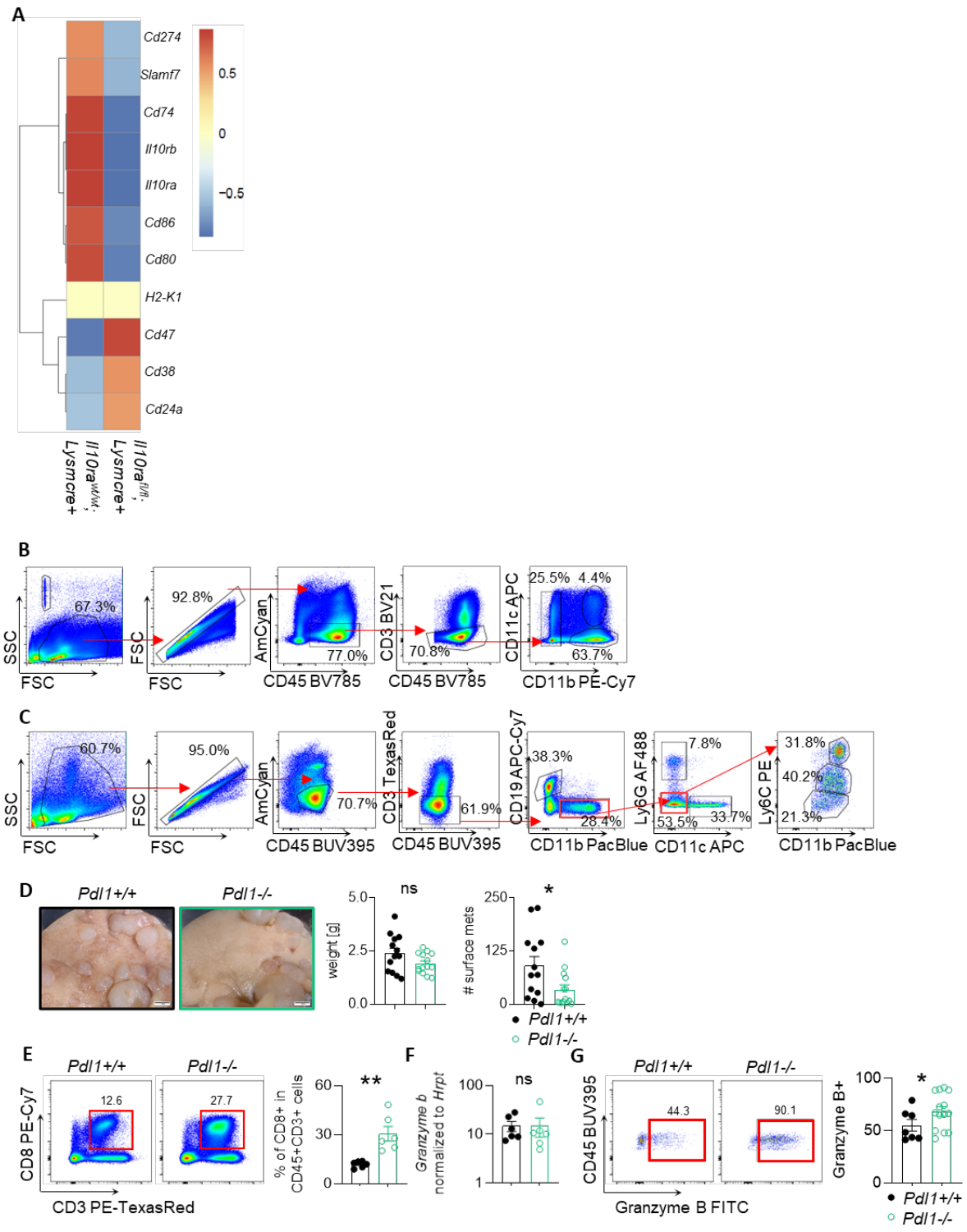

Fig. S7: PD-L1 deficiency enhances antitumor immunity of CD8+ T cells and reduces liver metastasis

(**A**) Bulk sequencing analysis on CD11b+ cells. (**B**) Gating strategy for Figure 6B. (**C**) Gating strategy for Figure 6C. (**D** to **G**) *Pdl1+/+* and *Pdl1-/-* mice were i.s. injected MC38 cancer cells (n ≥ 12 mice per group). (**D**) Livers were harvested 21 days post injection and metastatic burden was assessed. (**E**) 14 days post injection, representative FACS-plot and the frequency of hepatic CD8+ T cells, as well as

granzyme B level in CD8+ cells (**F**) before and (**G**) after coculture with MC38 cells *in vitro.* n ≥ 5 mice per group. Scale bar: 2 mm. Data are presented as mean ± SEM. Non-significant (ns): $p > 0.05$; *: $p \leq 0.05$; **: $p < 0.01$; ***: $p < 0.001$, as calculated by Mann-Whitney *U* test.

Supplementary materials and methods

LSEC isolation

The mice were euthanized and liver perfusion was performed, first by flushing with PBS, and then with 5 mL 0.05% collagenase into the portal vein and vena cava. The liver was sliced into small pieces and digested with 1 mg/ml collagenase and 10 U/ml DNase at 37°C for 25 minutes in RPMI (10% FBS, 1% pen/strep), while shaking. The remaining liver was filtered through a 200-µm cell strainer and cell isolation was performed by centrifuging twice at 40 g for 4 minutes and once at 400 g for 20 minutes. An Optiprep (Sigma, Kawasaki, Japan) gradient was used to enrich LSECs from theliver. For isolating LSECs, MACS sorting with anti-CD146 magnetic antibodies was used according to the manufacturer's protocol. LSECs were cultured on collagen-coated plates for 5 days before stimulation.

Extravasation assay

To perform the extravasation assay, the forced liver metastasis model was used as described above. Here, the difference was the time of euthanization and modified cancer cells. MC38 cells with a green fluorescent protein (MC38-GFP) were used for injections, and livers were harvested after 24 h. The livers were cut, digested and smashed into single cell resolution as mentioned above. Then, the supernatant was collected twice after a 40 g centrifuge for 4 mins. Next, cells in 1:10 dilution were mixed with counting beads (Spherotech Inc) for flow cytometry. A mouse injected with MC38shC cells was used as a negative control.

Fecal microbiome transfer

Stool was collected either from *C57BL/6J* mice (MB1) or from *Rag-/-(Yale)* mice with a colitogenic microbiome (MB2) [1]. Dissolved stool in brain heart infusion medium (Millipore) was transplanted into the recipient mouse using a gavage needle.

Mouse colonoscopy

A colonoscopy was performed to determine the severity of the colitis. The degree of colitis (scale 0-15) was determined as published [2], where 0 represents no colitis and 15 represents severe colitis. The mice were under isoflurane anesthesia, and the colonoscopy (Karl Storz) was performed once a week. Colitis severity was scored by two blinded investigators.

Western Blot

Cells were lysed in lysis buffer on a plate, then scraped and centrifuged at 14,000 g for 5 min. The supernatant was transferred to a new tube. Protein concentration was assessed using the NanoDrop-instrument. Protein samples were equalized with water and Laemmli buffer (60 µg/sample) and heated to 95°C for 5 min. Protein samples were run on a 10% Tris/Glyicine/SDS-PAGE, subsequently transferred from the gel to a PVDF-membrane using wet-blot electrophoresis for 60 min at 400 mA. The blotted membrane was incubated with blocking buffer (5% milk in PBS-T) for 1 hour, followed

by an incubation with antibody solution (1:1000 dilution) overnight at 4°C. The membrane was washed and incubated with the HRP-conjugated secondary antibody (1:2000) for 1 h. After washing, the blot was developed with chemiluminescent HRP substrate for 5 min before placing a film on the membrane (dark room). The photo film was run through a developer and the ladder was carefully marked on the film.

Bulk sequencing

To generate sequencing libraries, 2 mg RNA from each sample was used according to the manufacturer of NEBNext UltraTM RNA Library Prep Kit for Illumina (New England Biolabs, Ipswich, MA, USA). cDNA libraries were subsequently sequenced on Illumina HiSEquation 2500 yielding ~15 million 50 bp single-end reads per sample. To assess the RNA quality, FastQC v. 0.11.5 was used [3]. Alignment to mouse genome draft GRCm38.84 was conducted using STAR v. 2.5.0 [4]. For visualization and hierarchical clustering, using the transcripts per million method was used to normalize the reads, but raw read counts were used for differential expression analysis using DESeq2 v. 1.14 [5].

[1] **Palm NW, de Zoete MR**, Cullen TW, Barry NA, Stefanowski J, Hao L, et al. Immunoglobulin A coating identifies colitogenic bacteria in inflammatory bowel disease. Cell 2014;158:1000-1010.
[2] Becker C, Fantini MC, Wirtz S, Nikolaev A, Kiesslich R, Lehr HA, et al. In vivo imaging of colitis and colon cancer development in mice using high resolution chromoendoscopy. Gut 2005;54:950-954.
[3] Bolger AM, Lohse M, Usadel B. Trimmomatic: a flexible trimmer for Illumina sequence data. Bioinformatics 2014;30:2114-2120.
[4] Dobin A, Davis CA, Schlesinger F, Drenkow J, Zaleski C, Jha S, et al. STAR: ultrafast universal RNA-seq aligner. Bioinformatics 2013;29:15-21.
[5] Li B, Dewey CN. RSEM: accurate transcript quantification from RNA-Seq data with or without a reference genome. BMC Bioinformatics 2011;12:323.

Table S1: Taqman probes and primer sequences utilized for this study

gene	company	taqman probe/primer name	sequence (5' → 3')
		IL-10fw	GCC TTC AGT ATA AAA GGG GGA CC
		IL-10rev	GTG GGT GCA GTT ATT GTC TTC CCG
Il10-/-	Eurofins Genomics	IL10 neo	CCT GCG TGC AAT CCA TCT TG
		IL10fl 932	CCA GCA TAG AGA GCT TGC ATT ACA
Il10flox/flox	Eurofins Genomics	IL10fl 933	GAG TCG GTT AGC AGT ATG TTG TCC AG
		Foxp3 KI (F) 936	AGG ATG TGA GGG ACT ACC TCC TGT A
		Foxp3 KI (Rev) 937	TCC TTC ACT CTG ATT CTG GCA ATT T
		Foxp3 wt (F)	CCT AGC CCC TAG TTC CAA CC
Foxp3cre+	Eurofins Genomics	Foxp3 wt (Rev)	AAG GTT CCA GTG CTG TTG CT
		LysM Wt	TA CAG TCG GCC AGG CTG AC
		LysM common	CTT GGG CTG CCA GAA TTT CTC
Lysmcre+	Eurofins Genomics	LysM Mut	CCC AGA AAT GCC AGA TTA CG
		RagWF	GAG GTT CCG CTA CGA CTC TG
		RagR	CCG GAC AAG TTT TTC ATC GT
Rag-/-(Yale)	Eurofins Genomics	RagMF	TGG ATG TGG AAT GTG TGC GAG
		GFP-3	AAG TCG TGC TGC TTC ATG TG
		GFP-5	ACG TAA ACG GCC ACA AGT TC
		IL10KOF	GTG TGT ATT GAG TCT GCT GGA C
		IL10KOR1	GTG TGG CCA GCC TTA GAA TAG
Il10eGFP	Eurofins Genomics	IL10KOR2	GGT TGC CTT GAC CAT CGA TG
		FIR1	CAA AAC CAA GAA AAG GTG GGC
		FIR2	GGA ATG CTC GTC AAG AAG ACA GG
Foxp3RFP	Eurofins Genomics	FIR3	CAT CTT GGA GAG TCG GTG TG
		YAK235	ACT GCT GTA TCC CCT CAT CT
Il10raflox/flox		YAK236	GTG AGC GGA GAT TTT AAC AG
		Cdh5-Cre Fw	GTC CAA TTT ACT GAC CGT ACA C
Cdh5cre+	Eurofins Genomics	Cdh5-Cre Rev	CTG TCA CTT GGT CGT GGC AGC
		17AyfpF	CAA GTG CAC CCA GCA CCA GCT GAT C
		17AyfpRwt	CTT AGT GGG TTA GTT TCA TCA CAG C
Il17acre+	Eurofins Genomics	17AyfpCreR	GCA GCA GGG TGT AGG CAA TGC
		Rosa26 Seq1	AAA GTC GCT CTG AGT TGT TAT
		Rosa26 Seq2	GCG AAG AGT TTG TCC TCA ACC
a26floxSTOPflox YFP	Eurofins Genomics	Rosa26 Seq3	GGA GCG GGA GAA ATG GAT ATG
		63PC3CreF	TTC CCG CAG AAC CTG AAG ATG TTC G
Cd11ccre+	Eurofins Genomics	64PC3CreR	GCC AGA TTA CGT ATA TCC TGG CAG
		B7H1 P2	ATT GAC TTT CAG CGT GAT TCG CTT GTA G
		B7H1 P3	TTC TAT CGC CTT CTT GAC GAG TTC TTC TG
		B7H1 P1	AGA ACG GGA GCT GGA CCT GCT TGC GTT AG
Pdl1-/-	Eurofins Genomics	B7H1 P2	ATT GAC TTT CAG CGT GAT TCG CTT GTA G
Hprt	Thermo Fisher Scientific	Mm03024075_m1	
Il10	Thermo Fisher Scientific	Mm00439614_m1	
Il10ra	Thermo Fisher Scientific	Mm00434151_m1	
Il10rb	Thermo Fisher Scientific	Mm00434157_m1	
Granzyme B	Thermo Fisher Scientific	Mm00442837_m1	

Table S2: Flow cytometry antibodies utilized for this study

Antibody	Fluorochrom	company	Cat#	Clone	RRID
CD45	BV785	Biolegend	103149	30-F11	AB_2564590
CD45	BUV395	BD	564279	30-F11	AB_2651134
CD3	BV421	Biolegend	100228	17A2	AB_2562553
CD3	PE-Dazzle	Biolegend	100246	17A2	AB_2565883
CD3	BV650	Biolegend	100229	17A2	AB_11204249
CD3	BUV395	BD	740268	17A2	AB_2687927
CD4	APC	Biolegend	100412	GK1.5	AB_312697
CD4	BUV737	BD	612761	GK1.5	AB_2870092
CD8	PE-Cy7	Biolegend	100722	53-6.7	AB_312761
IL-10Ra	PE	Biolegend	112706	1B1.3a	AB_313519
Isotype	PE	Biolegend	400408	RTK2071	AB_326514
pSTAT3	BV421	Biolegend	651010	13A3-1	AB_2572088
PD-L1	BV711	Biolegend	124319	10F.9G2	AB_2563619
PD-1	BV421	Biolegend	135218	29F.1A12	AB_2561447
CD11b	PacBlue	Biolegend	101224	M1/70	AB_755986
CD11c	APC	Biolegend	117312	N418	AB_389328
Ly6G	AF488	Biolegend	127625	1A8	AB_2561339
Ly6C	PE	Biolegend	560592	AL-21	None availiable
CD19	APC-Cy7	Biolegend	115530	6D5	AB_830707
Fixable Viability Dye eFluor 506	BV510	Invitrogen	65-0866-14	ıg doesnt target a spe	None availiable
PI	PE	Invitrogen	P1304MP	/	None availiable
Annexin	APC	Biolegend	640920	/	None availiable
TNFa	BV421	Biolegend	506328	MP6-XT22	AB_2562902
Granzym B	FITC	BioLegend	515403	GB11	AB_2114575